J Incl Phenom Macrocycl Chem (2013) 75:57–68
DOI 10.1007/s10847-012-0146-4

ORIGINAL ARTICLE

Spectral modulation of a charge transfer reaction of 2-methoxy-4-(*N*,*N*-dimethylamino)benzaldehyde inside cyclodextrin nanocage

Anuva Samanta · Sankar Jana · Nikhil Guchhait

Received: 3 May 2011 / Accepted: 12 March 2012 / Published online: 13 May 2012

Abstract This article reports modulation of intramolecular charge transfer (ICT) reaction of 2-methoxy-4-(*N*,*N*-dimethylamino)benzaldehyde (2-MDMABA) encapsulated within the cyclodextrin nanocavities investigated by steady state and time resolved measurements. The ICT emission, absent in bulk water, originates in the presence of α-, *β*- and *γ*-CD with the huge enhancement of local emission. From the Benesi–Hildebrand plot, the stoichiometry of the host–guest inclusion complex is found to be 1:1 for *β*- and *γ*-CD whereas 1:1 and 1:2 guest to host complexation occur at low and high concentration of α-CD, respectively. The association constants of the inclusion complexes have also been estimated from the Benesi–Hildebrand plot. The greater binding capability of 2-MDMABA with *β*-CD than that of other two CDs is further supplemented by time resolved study.

Keywords Intramolecular charge transfer · Cyclodextrin · Scanning electron microscope · Benesi–Hildebrand plot · Density functional theory

Introduction

The studies of photoreactions inside the nanocavities embrace virtually all field of chemistry [1–7]. Cyclodextrins (CDs) are indispensable excipients in many scientific areas such as pharmacy, environment, synthetic and analytical chemistry, for extraction of natural products [2]. They also serve as an excellent miniature replica for enzyme-substrate complex [8, 9]. Natural cyclodextrins are manufactured from starch by the action of cyclodextrin glucanotransferase (CGTase), an enzyme produced by several organisms, *Bacillus macerans* being the earliest source [4]. Cyclodextrins are water soluble α-1,4-linked cyclic oligomers of glucopyranose ($C_6H_{10}O_5$) units arranged in a toroidal structure. The most available three distinct CDs consist of six, seven or eight glucopyranose units and are named as α-CD (cyclohexaamylose), *β*-CD (cycloheptaamylose) or *γ*-CD (cyclooctaamylose), respectively. Internal diameter of the cavity accessible to the guest molecule varies as 4.5, 7.8 and 9.5 Å for α-, *β*- and *γ*-CD, respectively [2, 9]. The height of the torus of all the CDs is more or less the same and is about 7.9 Å [2]. CDs are shaped like truncated cones having a smaller and larger rim (Scheme 1). They have special molecular structure with a hydrophilic outer surface and a hydrophobic inner cavity that has the ability to sequester lipophilic molecules of appropriate size in aqueous and non-aqueous solution. The guest molecules are stabilized within the cavity by hydrophobic force without forming any covalent bonds and also by the hydrogen bond formation with the glucose hydroxyl groups at both the rims of the CD cavity [10]. The hydrophobic interior and the restricted geometry provided by the CDs exert a profound effect on the physicochemical properties of guest molecules if they are temporarily locked or caged within the host cavity.

The encapsulation ability of CDs has innumerable applications in the scientific fields such as drug design, food chemistry, water purification, ion exchangers, catalysts in chemical reactions [1, 11–13]. The inclusion phenomenon can be investigated by spectrophotometric and fluorimetric measurements as shielding of the guest molecules from outer environments deactivates non-radiative decay channels thereby enhancing their fluorescence intensity. So emissive behavior of the guest molecule entrapped in CDs cavity is affected and many significant

A. Samanta · S. Jana · N. Guchhait (✉)
Department of Chemistry, University of Calcutta, 92 A.P.C. Road, Kolkata 700009, India
e-mail: nguchhait@yahoo.com

Scheme 1 Chemical structure and shape of different cyclodextrins

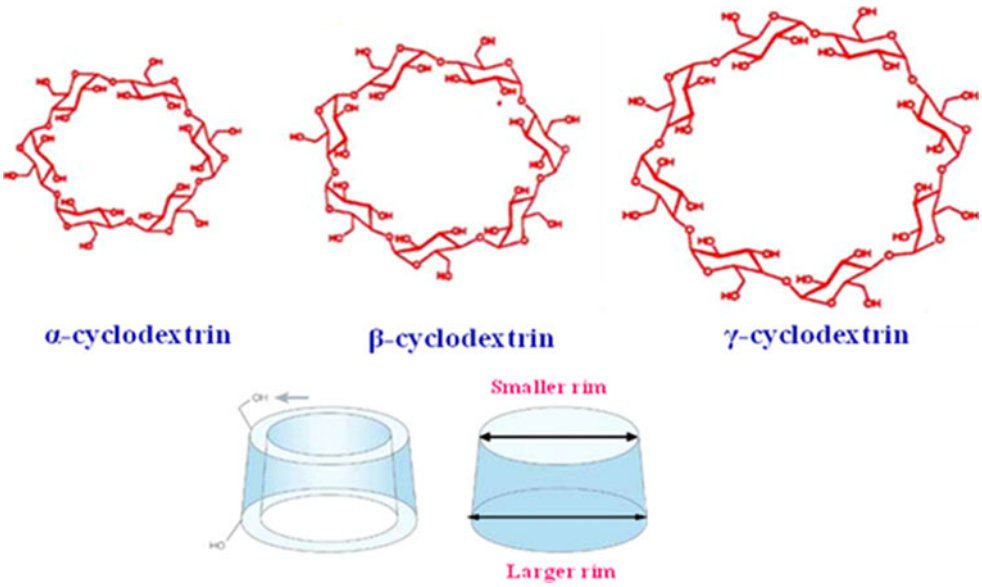

photochemical processes, such as excited state intramolecular proton transfer (ESIPT) [14–16], intramolecular charge transfer (ICT) [17–20], dimer and excimer formation [21, 22], have been successfully examined.

There are several molecules containing donor–acceptor groups exhibiting ICT phenomenon in the excited state [23, 24]. One of the most extensively studied molecule capable for charge transfer process in the excited state is 4-(*N*,*N*-dimethylamino)benzonitrile (DMABN) [25, 26]. This ICT molecule shows short wavelength emission band recognized as locally excited (LE) state along with a long wavelength ICT band originating from a state with a perpendicular conformation. Recently, we have reported the steady state spectra of 2-methoxy-4-(*N*,*N*-dimethylamino)benzaldehyde (2-MDMABA) in solvents of varying polarity and hydrogen bonding capability [27]. The photophysical behavior of this probe is more or less similar with its parent molecule, 4-(*N*,*N*-dimethylamino)benzaldehyde (DMABA) [28, 29], as it shows π–π^* absorption band at $\sim$340 nm and strong LE at $\sim$385 nm and weak ICT emission at $\sim$520 nm in polar aprotic solvents, similar to that of DMABA. Since solvent polarity shows marked influence on the ICT fluorescence of DMABA and 2-MDMABA, these molecules can be utilized as a probe to study their encapsulation behavior inside the cyclodextrin cavity. Encapsulation of DMABA in α-CD and β-CD has been reported previously by Chattopadhyay et al. [30, 31]. This article is an attempt to explain the different complexation susceptibility of synthesized 2-MDMABA within different CD cavities based on characteristic changes in LE and CT emission. In this context, here we would like to focus the efficiency of 2-MDMABA as a potential fluorescence probe for understanding its interaction with different host molecules.

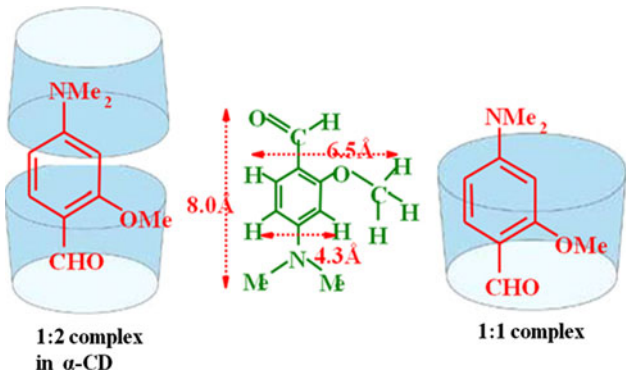

Scheme 2 Optimized geometry of minimum energy conformer of 2-MDMABA calculated at DFT/B3LYP/6-31 ++G** level. The proposed 1:2 and 1:1 inclusion complexes in α- and β-CD (*right*) respectively

Experimental section

Reagents

The target compound 2-MDMABA (Scheme 2) was synthesized as described in our previous publication [27]. α-CD was obtained from Himedia, India and β- and γ-CD were purchased from Sigma, Aldrich. Triple distilled water was used for the preparation of aqueous solution. Analytical grade H_2SO_4 from Merck was used as received.

Fluorescence and UV–Vis absorbance

The room temperature absorption and steady state fluorescence spectra were recorded using Hitachi UV–Vis U-3501 spectrophotometer and PerkinElmer LS-55 fluorimeter, respectively. Temperature variation fluorescence

spectra have been measured by keeping the emission cell compartment at a chosen temperature using variable temperature chiller. In all measurements, the concentration of 2-MDMABA has been maintained within the range 10^{-5}–10^{-6} mol/dm^3 in order to avoid dimerization. Steady state fluorescence anisotropy r was measured using fluorimeter mentioned above. The anisotropy is defined by

$$r = \frac{(I_{VV} - GI_{VH})}{I_{VV} + 2GI_{VH}} \quad (1)$$

Here, I_{VV} and I_{VH} are the emission intensities obtained with the excitation polarizer oriented vertically and emission polarizer oriented vertically and horizontally, respectively. The G factor is the ratio of sensitivities of detection systems for vertically and horizontally polarized light $G = I_{HV}/I_{HH}$.

The fluorescence quantum yields were estimated from the corrected fluorescence spectra using quinine sulfate in 0.1 M H_2SO_4 ($\Phi_F = 0.577$ at 293 K) as secondary standard [32].

Fluorescence lifetime measurements

All the fluorescence decays were obtained with a Time Correlated Single Photon Counting (TCSPC) set up employing a nanosecond diode laser (IBH, nanoLED-07) operating at $\lambda_{ex} = 340$ nm as the light source and TBX-04 as the detector [33]. Instrument response function is 45 ps. Fluorescence decay was collected with an emission polarizer kept at the magic angle ($\sim$54.7°). The decays were analyzed using Data Station v-2.5 decay analysis software. The fluorescence decay curves were analyzed by bi- and tri-exponential fitting program of IBH in order to obtain best residuals and acceptable χ^2 values. Intensity decay curves were obtained as a sum of exponential terms

$$F(t) = \sum_i a_i \exp\left(\frac{-t}{\tau_i}\right) \quad (2)$$

where $F(t)$ is the fluorescence intensity at time t, a_i the pre-exponential factor representing the fractional contribution to the time resolved decay of the ith component with a lifetime τ_i. Average lifetimes (τ_{avg}) of fluorescence were calculated from the decay times and pre-exponential factors using the following equation:

$$\tau_{avg} = \sum_i a_i \tau_i \quad (3)$$

Scanning electron microscope measurements

To observe the morphology of the free 2-MDMABA, free CD and CDs + 2-MDMABA complex, the scanning electron micrographs were taken using a scanning electron microscope (SEM), Hitachi S3400N, Japan, with SE mode applying an accelerating voltage of 15 kV. One tiny drop of each 50 μM 2-MDMABA, 20 mM α-CD, 15 mM β-CD and their corresponding inclusion complex solutions were placed on 5 × 5 × 1 mm glass slide and were dried in vacuum and kept overnight for taking SEM. The prepared samples were placed on a sample studs and coated with gold by ion sputtering.

Results and discussion

Absorption study

The basic photophysics of the target 2-MDMABA molecules has been reported in our previous publication [27]. In aqueous medium, 2-MDMABA shows absorption maximum around $\sim$351 nm [27], originated from π–π* type of transition. Figure 1 delineates the absorption spectra of 2-MDMABA in aqueous solution containing different concentration of CDs. On addition of α-CD, the absorption maxima of the lowest energy band shifts to longer wavelength from $\sim$351 to $\sim$354 nm (Fig. 1a). This change in absorption could be attributed to the penetration of the probe inside the hydrophobic cavity directing towards the formation of complexes between α-CD and 2-MDMABA. Similar to α-CD, addition of β-CD to aqueous solution of 2-MDMABA exhibits the same result (Fig. 1b). The higher wavelength absorption band is red shifted by 3 nm. So this change in absorbance upon addition of CDs may be approved to the formation of inclusion complexes. It is to note that we did not observe significant changes in case of γ-CD.

Emission study

As reported in our recent work [27], 2-MDMABA shows distinct dual emission in polar aprotic solvents. The higher energy emission ($\sim$385 nm) has been assigned to be arising from the LE state whereas CT emission arises at $\sim$520 nm. In pure water, the ICT emission of 2-MDMABA is hardly observed. It yields almost a single fluorescence of LE state with a maximum at $\sim$411 nm [27], but no well resolved CT emission could be observed. In addition to the decrease in energy of the CT state by dielectric stabilization, the intermolecular hydrogen bonding interaction with water opens up usual non-radiative channels. It is proposed that the stabilization of the CT state reduces the energy gap between the ICT state and the Franck–Condon state resulting in a rapid non-radiative decay of the ICT state to the low-lying triplet state [27]. That may be the reason of observing only LE emission in protic solvents. With addition of α-CD, a new fluorescence band around $\sim$520–530 nm starts to grow up along with

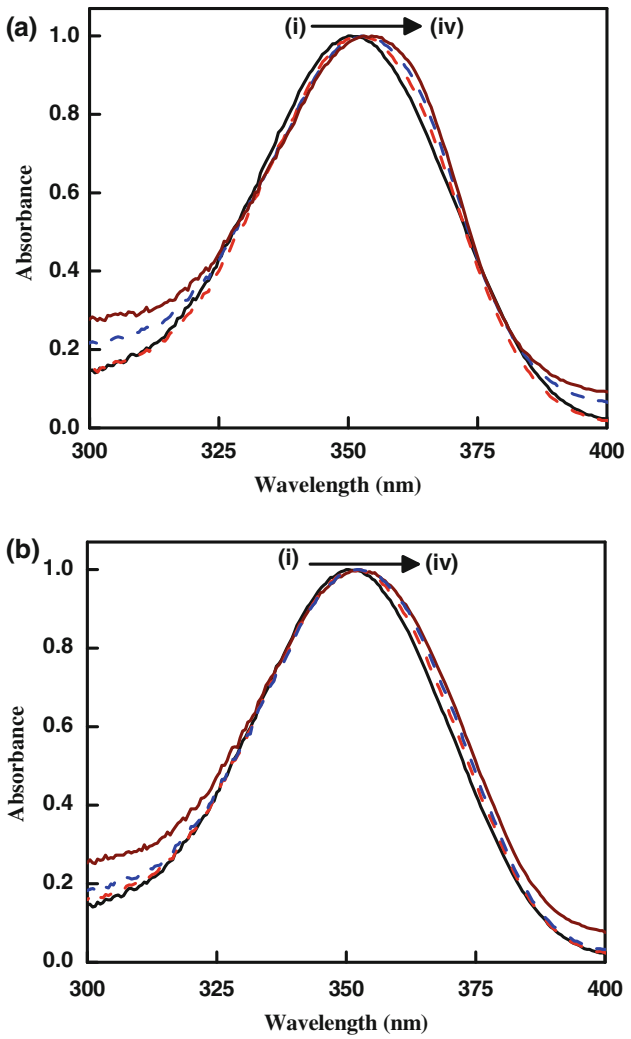

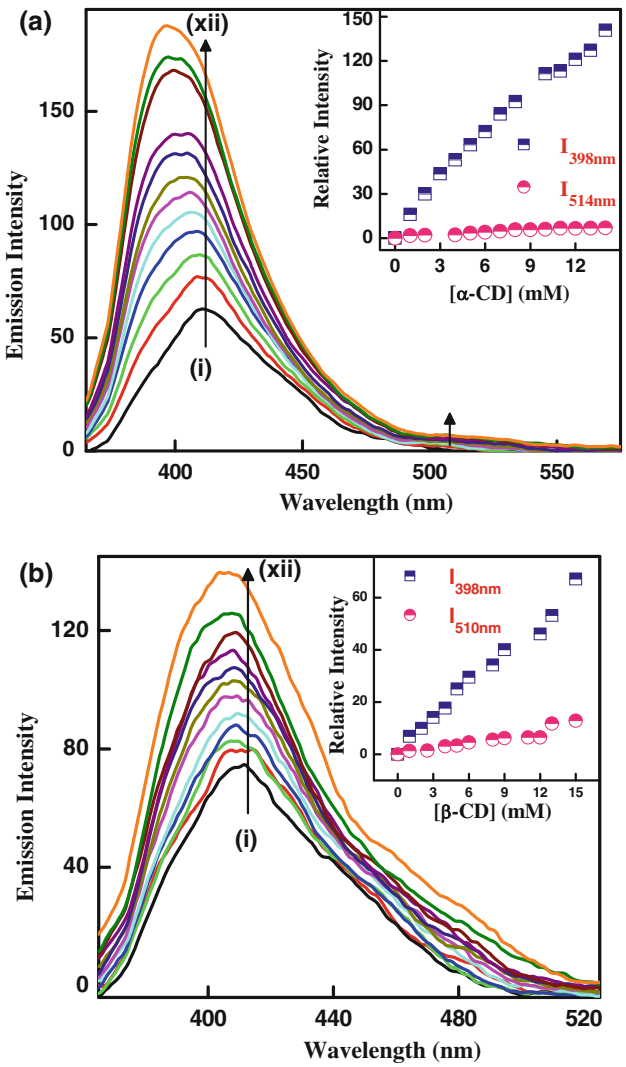

Fig. 1 Absorption spectra of 2-MDMABA (4 μM) in aqueous solutions with varying concentrations of **a** α-CD ((i) → (iv) correspond to 0, 5, 10, 20 mM of α-CD), **b** *β*-CD ((i) → (iv) correspond to 0, 5, 10, 15 mM of *β*-CD)

the intensity enhancement of the normal fluorescence band (Fig. 2a). The LE band shows a blue shift (∼14 nm) with increase of α-CD concentration up to 14 mM without further remarkable clear shift of the ICT band (Table 1). The change in intensities with increase in α-CD concentration for both the LE (398 nm) and CT (514 nm) band are shown in inset of Fig. 2a. The effect of *β*-CD on the aqueous solution of 2-MDMABA demonstrates the similar results and has been depicted in Fig. 2b. Here also, the LE emission band exhibits a huge intensity enhancement compared to the ICT band with little blue shifting of the maximum position from ∼411 to ∼404 nm. In case of *γ*-CD, the corresponding changes are very trivial as shown in Fig. 2c. The relative changes in the position maximum of LE emission has been portrayed in Fig. 3a. The corresponding enhancement of the local emission band is high compared to the ICT band as shown in inset of Fig. 2. The increase in intensity of the LE band is due to the encapsulation of 2-MDMABA in the hydrophobic cavity of CDs. The

◀ **Fig. 2** Fluorescence emission spectra (λ_{ex} = 350 nm) of 2-MDMABA (4 μM) in water on the addition **a** α-CD ((i) → (xii) correspond to 0, 1, 2, 3, 4, 5, 6, 7, 8, 12, 13, 14 mM of α-CD), **b** β-CD ((i) → (xii) correspond to 0, 1, 2, 3, 4, 5, 6, 8, 9, 12, 13, 16 mM of β-CD), **c** γ-CD ((i) → (vii) correspond to 0, 2, 3.5, 5, 6, 8, 10 mM of γ-CD). Inset shows the plot of fluorescence intensities at LE and ICT band maxima versus [CD] for 2-MDMABA complexed to CDs

emergence of ICT emission band of 2-MDMABA in aqueous CDs solution can be explained in terms of the polarity reduction of the guest affected by CD encapsulation. The ICT state of 2-MDMABA forms hydrogen bond with highly polar water, thereby stabilizes this state by lowering its energy level. Thus the probability of non-radiative decay of CT state through internal conversion or intersystem crossing, increases and consequently a decrease in the fluorescence of CT band occur. It is known that hydrophobicity is the main driving force in aqueous cyclodextrin solution for encapsulation of the molecule inside the cavity interior [14–20]. Therefore, it is expected that the $-NMe_2$ group of 2-MDMABA will be projected toward the bulk aqueous phase and the slightly hydrophobic formyl (–CHO) residue would like to entrap inside the deep core of the non-polar cavity. In that case, formation of hydrogen bond between C=O group of 2-MDMABA and water is discarded as no water molecule would be available to C=O group inside the cavity. So the rate of non-radiative decay decreases causing an enhancement of the CT band.

On the basis of the fluorescence spectra shown in Fig. 2, we could estimate the quantum yield at different concentration of CDs and the corresponding data has been collected in Table 1 and Fig. 3b. With increasing CDs concentration the Φ_F values of 2-MDMABA increases supporting the above discussed decrease of non-radiative decay rates. The extent of blue shift as well as increase of Φ_F values in α-CD is more compared to that caused by β-CD and γ-CD. The excitation spectra monitored at the emission maxima, shown at Fig. 3c, are found to be well matched with the absorption spectra showing red shifting of the excitation spectra with increasing concentration of CDs. This observation infers that the emitting state has the same origin and a single type of equilibrium is present in the host–guest mixed system.

Stoichiometry and association constant of host–guest equilibrium

In order to achieve a quantitative estimation of binding between 2-MDMABA and CDs, binding constant has been determined from the fluorescence intensity data following the well used Benesi–Hildebrand equation. The complexation reaction with equilibrium constant can be expressed as follows

$$2-\text{MDMABA} + \text{CD} \rightleftarrows 2-\text{MDMABA} : \text{CD}$$

$$K = \frac{[2-\text{MDMABA} : \text{CD}]}{[2-\text{MDMABA}][\text{CD}]} \tag{4}$$

where K is the binding constant in M^{-1}. The concentration terms of each component of Eq. 4 can be expressed in terms of fluorescence intensity. Assuming the concentration of the probe–CD complex is very low compared to that of the free CD, the Benesi–Hildebrand relation for these types of complexation process can be written as follows:

$$I = \frac{I_0 + I_1 K[\text{CD}]}{1 + K[\text{CD}]}$$

Rearranging the above equation we have:

$$\frac{1}{(I - I_0)} = \frac{1}{(I_1 - I_0)} + \frac{1}{(I_1 - I_0)K[\text{CD}]} \tag{5}$$

where I_0, I and I_1 are the emission intensities in absence, at intermediate and infinite concentration of CD, respectively. As shown in Fig. 4, the Benesi–Hildebrand double reciprocal plot ($1/(I-I_0)$ vs. 1/[CD]) yields a straight line justifying 1:1 complexation between the fluorophore and CDs, whereas the variation of $1/(I-I_0)$ versus $1/[CD]^2$, considering 1:2 complex, does not show a straight line in case of β-CD (Fig. 4b). The above results authenticate that if 1:1 complex formation is ensured between 2-MDMABA and CDs and the corresponding binding constant is to be 61.2 ± 3.4, 76.0 ± 3.3 and 7.0 ± 1.8 M^{-1} for α-, β- and γ-CD, respectively (Table 1). It is evident that 2-MDMABA binds stronger with β- and α-CD compared to γ-CD. But at higher concentration of α-CD, the plot of $1/(I-I_0)$ versus $1/[CD]^2$ yields a straight line suggesting 1:2 complexation (inset of Fig. 4a) with 8.78×10^3 M^{-2} binding constant value. The greater degree of blue shifting as well

Table 1 Spectral characteristics of 2-MDMABA in various environments

Medium	λ_{abs} (nm)	λ_{em} (nm)	Φ_F (x10^5)	Stoichiometry	Binding constant (K)
Water	351	411	5.7	–	–
α-CD (20 mM)	354	397, 520	27.3	1:1	61.2 ± 3.4 M^{-1}
				1:2	8780 ± 230 M^{-2}
β-CD (15 mM)	354	404, 520	14.3	1:1	76.0 ± 3.3 M^{-1}
γ-CD (10 mM)	351	410, 520	7.7	1:1	7.0 ± 1.8 M^{-1}

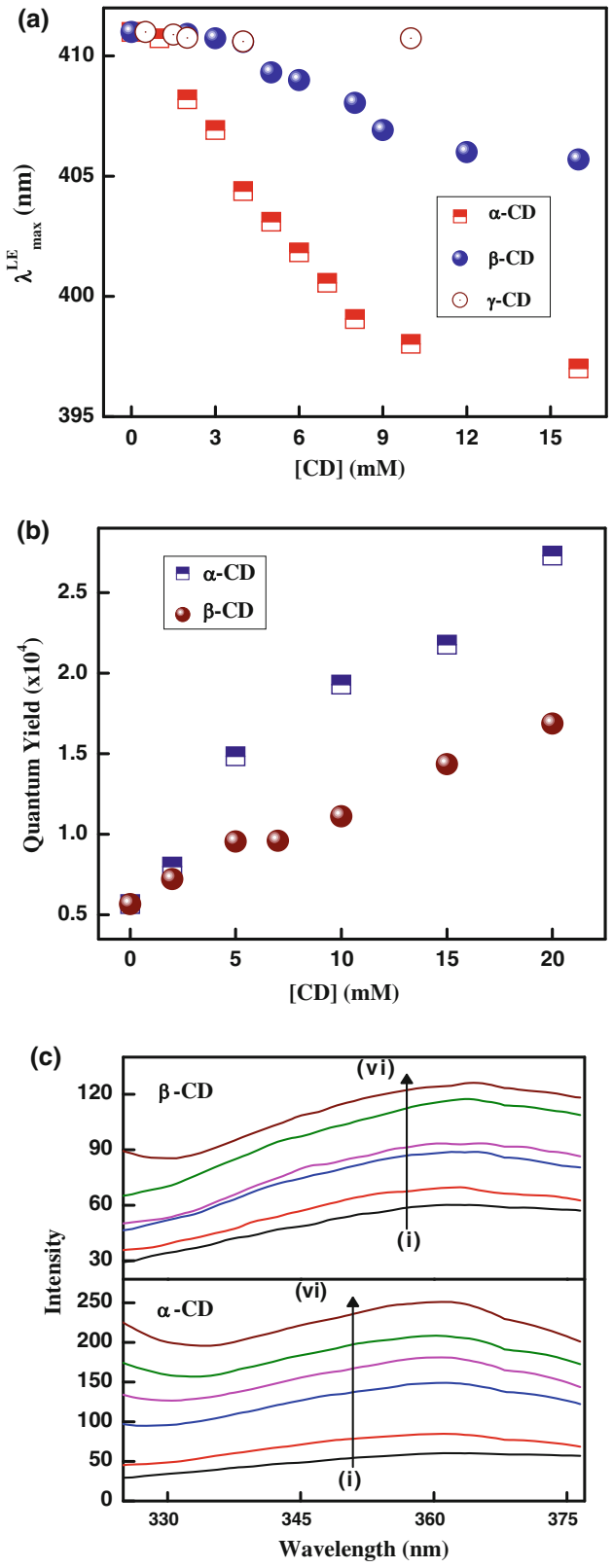

as high fluorescence quantum yield can be explained in terms of 1:2 complexation between α-CD (higher concentration) and 2-MDMABA. From theoretical structural

◀**Fig. 3** **a** Plot of fluorescence band maxima of LE and **b** fluorescence quantum yield values against concentration of CDs. **c** Fluorescence excitation spectra monitored at 410 nm of 2-MDMABA (4 μM) in the presence of increasing concentration of *β*-CD ((i) → (vi) correspond to 0, 2, 5, 7, 10, 15 mM of *β*-CD) and α-CD ((i) → (vi) correspond to 0, 2, 5, 10, 15, 20 mM of α-CD)

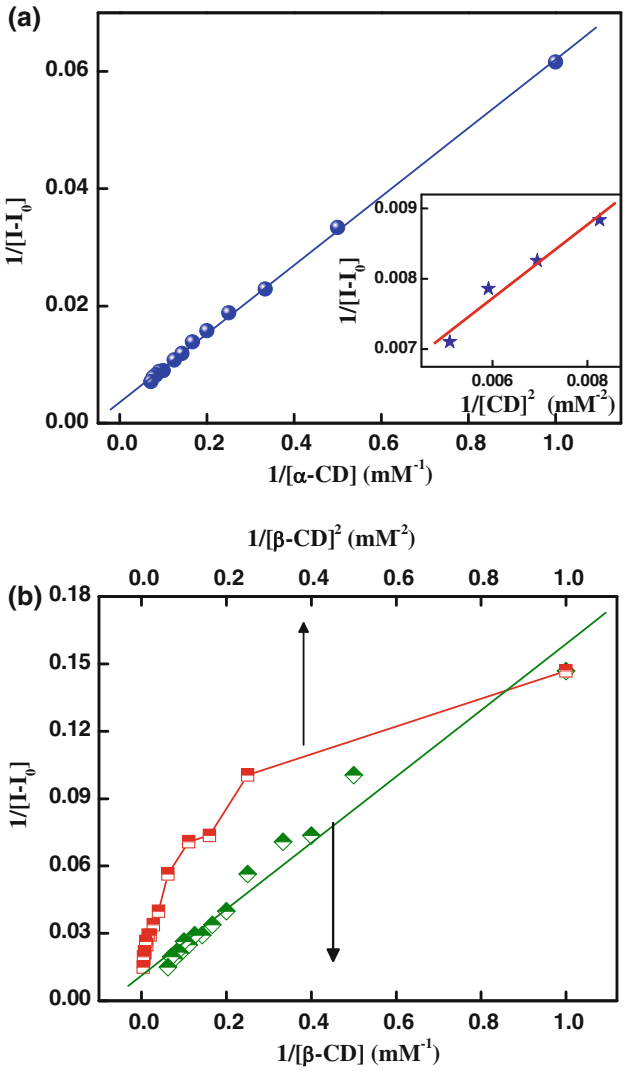

Fig. 4 Benesi–Hildebrand plot for 2-MDMABA (4μM) complexed to **a** α-CD for 1:1 complexation (*inset* shows 1:2 complexation of α-CD at higher concentration) and **b** *β*-CD assuming 1:1 and 1:2 stoichiometries

calculation of 2-MDMABA at DFT/B3LYP/6-31++G** level using Gaussian 03 software [34], the different end to end distance of the probe molecule have been presented in Scheme 2. For the acceptor group side, the end to end distance is 6.5 Å, so 2-MDMABA can enter partially into the α-CD cage as the diameter of α-CD is 4.5 Å. So, another cyclodextrin cage is necessary for complete encapsulation of the probe molecule inside α-CD. From the determined *K* value, the free energy change ($\Delta G = -RT\ln K$) for the probe-CD binding process has been

calculated to be −10.2 kJ/mol (−22.5 kJ/mol for 1:2) and −10.7 kJ/mol for α- and β-CD, respectively, which indicates spontaneous complexation process.

Steady state fluorescence anisotropy study

Steady state fluorescence anisotropy (r) study has always occupied a position of central importance in biochemical and biophysical research because of its tremendous ability to produce valuable information about the environment in the direct vicinity of the fluorophore, since the microenvironment of the probe molecule is governed by its precise location in the molecular assembly. Any modulation in the rigidity of the surrounding environment of the fluorophore, like shape, size, and flexibility etc. affects the observed anisotropy. The so-called environment induced motional restriction imposed on the mobility of the probe by its microenvironment is manifested through anisotropy variation and thereby furnishing clues to assess the probable location of the probe in the microheterogeneous environments like cyclodextrins, proteins, DNA, micelles etc. [35]. Since encapsulation phenomenon occurs between 2-MDMABA and CDs, the restricted motion of the $-NMe_2$ group in aqueous solution of CDs can be corroborated well by steady state anisotropy measurements. The plot of variation of fluorescence anisotropy of 2-MDMABA as a function of α-, β- and γ-CD concentration is shown in Fig. 5. In all the cases, huge enhancement of fluorescence anisotropy with increasing concentration of CDs is observed. This result can be attributed to significant restriction imposed on the rotational motion of the molecule. However, the anisotropy value is higher in case of α-CD (higher concentration) probably due to the greater binding aptitude of 2-MDMABA within α-CD cavity.

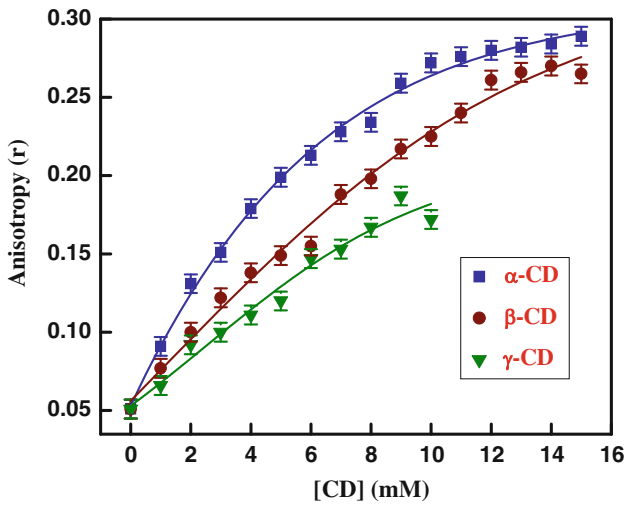

Fig. 5 Variation of fluorescence anisotropy (r) of 2-MDMABA (4 μM) with increasing concentration of different CDs in aqueous medium

Temperature effect

Temperature has profound effect upon complexes as it can destabilize the inclusion complex. Once an inclusion complex is formed by displacing the solvent molecules from the CD cavity, it exhibits long and stable self life until it is heated. With increase of temperature, stability of the inclusion complex decreases by the displacement of the guest molecules by water molecules. So temperature can influence the emission behavior of CD-2-MDMABA complexation. The aqueous solution of α-CD-2-MDMABA complex is subjected to change of temperature from 20 to 70 °C as shown in Fig. 6a. The LE emission band sensibly decreases whereas the decrease of ICT emission is extremely low. As displayed in Fig. 6b, the ratio of emission intensity of LE and CT bands decreases from 21.7 to 14.7 showing greater change of LE emission intensity. The emission maximum of the LE band also shifts from ∼401 to ∼409 nm. The red shift and decrease in fluorescence intensity indicate that the polarity of the environment around the probe increases. As the inclusion complex gets disrupted due to increase of temperature, the probe molecules encapsulated within the hydrophobic cavity of CD are relocated to the aqueous phase. Inset of Fig. 6a reflects the opposite pattern of Fig. 3a. This exposure of the probe molecules in the bulk aqueous phase rejuvenates the non-radiative decay channels thereby exhibiting red shifting and intensity reduction.

Time resolved study on host–guest equilibrium

Fluorescence lifetime serves as a sensitive indicator of the local environment in which a given fluorophore is placed. So this fluorescence technique could provide valuable information regarding the location and distribution of a probe in complex microheterogeneous environments such as protein, micelle, lipid, cyclodextrin etc. in a better way. To develop a better view about the changes in the photophysics of the probe molecule engaged in the CD cavity, we performed time resolved fluorescence experiment. The LE emission maximum (410 nm) of the probe is monitored due to the absence of CT state in water and 2-MDMABA shows bi-exponential decays. On the other hand in CDs solution, the decay pattern is more complicated and is best fitted by tri-exponential decay. Figure 7 displays the decay profile of 2-MDMABA in water and in different CDs environment. Since the decay profiles of inclusion complexes are multi-exponential in nature, it is very difficult to predict the contribution of each component. In order to simplify it, we prefer to use average fluorescence lifetime

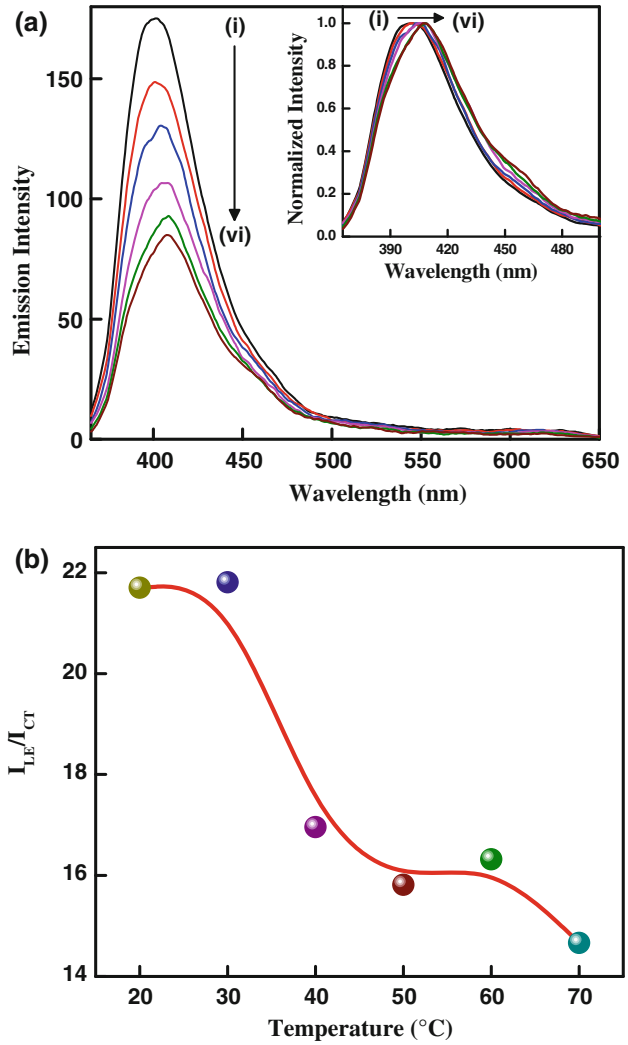

Fig. 6 **a** Temperature dependence of the fluorescence emission (λ_{ex} = 350 nm) of 2-MDMABA (4 μM) in the presence of 20 mM α-CD in water, curves (i) → (vi) correspond to 20, 30, 40, 50, 60 and 70 °C. Inset: normalized emission spectra of 2-MDMABA in 20 mM α-CD with increasing temperature from 20 to 70 °C. **b** Temperature dependence of the LE/CT emission intensity ratio of 2-MDMABA complexed with 20 mM α-CD

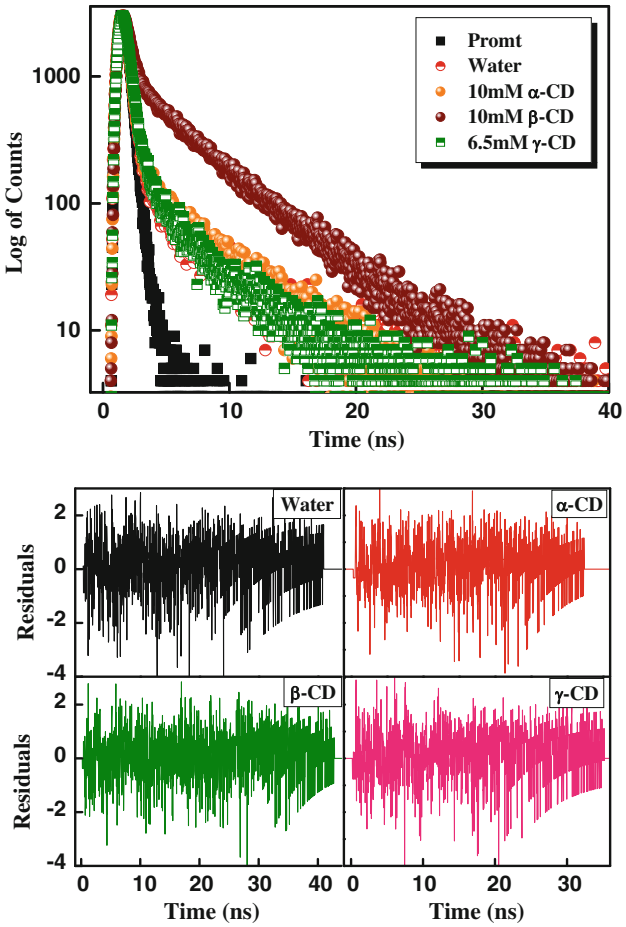

Fig. 7 Emission decay traces of 2-MDMABA (4 μM) in aqueous and aqueous CD solutions ([α] = [β] = 10 mM and [γ] = 6.5 mM) with λ_{ex} = 340 nm and λ_{em} = 410 nm. The corresponding best fitted residuals with acceptable χ^2 have been also shown

(τ_{avg}) as determined using Eq. 3 and the values are listed in Table 2. The average lifetime of 2-MDMABA in water is 0.054 ns. Adding 10 mM α-CD to this solution increases the lifetime to 0.059 ns. Upon addition of 2-MDMABA into 10 mM β-CD aqueous solution, this decay time is further increased to 0.126 ns. So the fluorescence lifetime values of the probe in cyclodextrin media are clearly longer than those in water due to decrease in non-radiative decay rates and the probe is in the restricted environment. The radiative (κ^r) and non-radiative (κ^{nr}) decay rate constants (Table 2) are calculated using the following equations:

$$\kappa^r = \Phi_F/\tau_{avg} \qquad \kappa^{nr} = (1-\Phi_F)/\tau_{avg} \tag{6}$$

Table 2 Fluorescence lifetime, radiative and non-radiative rate constants of 2-MDMABA in aqueous and aqueous CD nanocage

Medium	τ_1 (ns)	τ_2 (ns)	τ_3 (ns)	τ_{avg} (ns)	χ^2	$k^r \times 10^{-7}$ (s^{-1})	$k^{nr} \times 10^{-9}$ (s^{-1})
Water	2.009 (0.2%)	0.051 (99.8%)	–	0.054 ± 0.001	1.16	0.106	18.52
α-CD (10 mM)	1.595 (0.17%)	5.668 (0.18%)	0.047 (99.65%)	0.059 ± 0.003	1.03	0.327	16.94
β-CD (10 mM)	1.970 (0.69%)	5.690 (1.11%)	0.050 (98.2%)	0.126 ± 0.010	0.92	0.114	7.93
γ-CD (6.5 mM)	1.397 (0.44%)	5.780 (0.14%)	0.051 (99.42)	0.064 ± 0.005	1.08	0.120	15.62

Numbers in the brackets represent the corresponding relative amplitudes of different components in bi- and tri-exponential fitting of the profiles

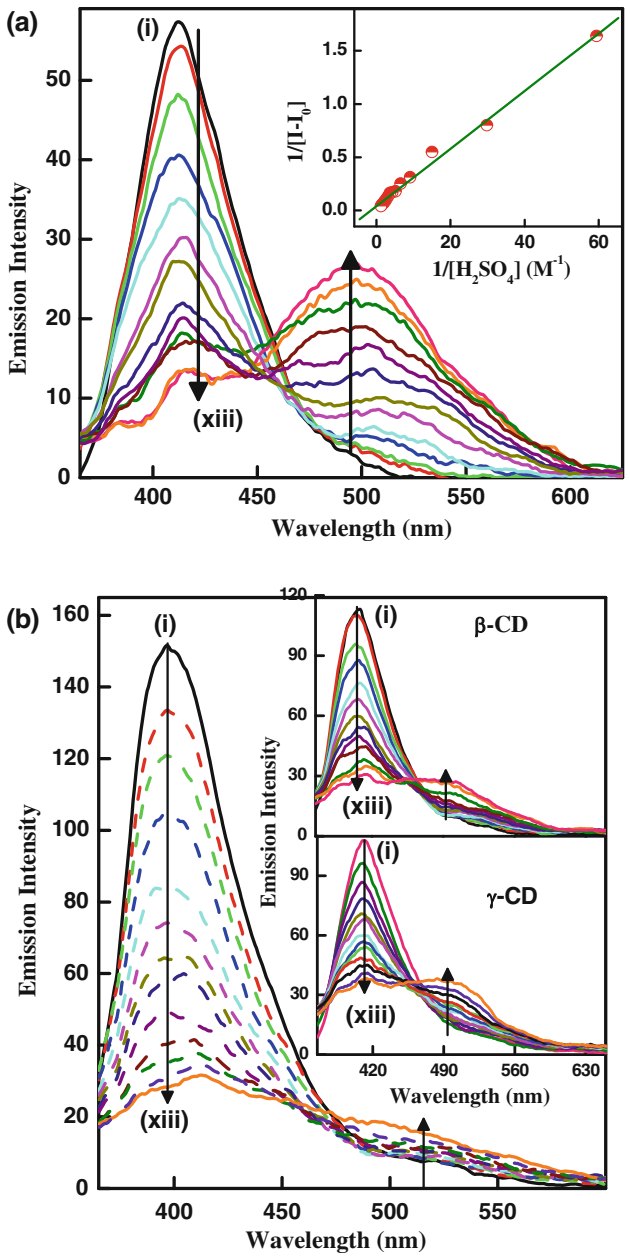

Fig. 8 **a** Variation of emission spectra (λ_{ex} = 350 nm) of 2-MDMABA (3 μM) in aqueous solution with varying concentration of H_2SO_4; curves (i) → (xiii) correspond to $[H_2SO_4] = 0$ to 0.79 M. *Inset* shows Benesi–Hildebrand plot exhibiting 1:1 equilibrium maintained between neutral and monoprotonated species. **b** Effect of acid on the emission spectra (λ_{ex} = 350 nm) of 2-MDMABA (4 μM) in aqueous solution of 10 mM α-CD. (i) → (xiii) present $[H_2SO_4] = 0$ to 0.79 M. Inset shows the effect of H_2SO_4 on the emission spectra (λ_{ex} = 350 nm) of 2-MDMABA complexed with aqueous solution 10 mM *β*-CD and 10 mM *γ*-CD with variation of concentration of H_2SO_4 from 0 to 0.79 M, respectively

The increase in Φ_F (Table 1), decay times (Table 2) and substantial decrease in κ^{nr} in the cyclodextrin interior point to the restricted motion of the probe inside the cyclodextrin cavities. As seen in Table 2, the decay times increase in the order: water < α-CD < *γ*-CD < *β*-CD and non-radiative rate constants decrease as follows: water > α-CD > *γ*-CD > *β*-CD. Similar to binding constant values, the lifetime datum also supports the compact packing of the probe inside the *β*-CD nanocage.

The comparatively lower blue shifting, lower increase of Φ_F and lower lifetime values for *γ*-CD than that for *β*-CD may be explained in terms of greater cavity size of *γ*-CD (9.5 Å), which outcomes in a loosely bound complex with 2-MDMABA as the corresponding end to end distance of the probe has been depicted in Scheme 2. So this loose-fitting by *γ*-CD results that the entry of water molecules is not completely restricted where in *β*-CD, the entry of water molecules into the encapsulated center is completely forbidden. Reactivation of the non-radiative decay channels within *γ*-CD cavity may be the main cause for its different behavior during the encapsulation phenomenon.

Effect of variation of pH

It is found that donor acceptor charge transfer systems show blue shifted absorption and emission in presence of acid due to the formation of protonated species. The H^+ ion of acid binds to the lone pair of nitrogen of donor and hence CT emission decreases due to unavailability of lone pair. Figure 8a portrays the effect of acid on the emission spectra of 2-MDMABA in aqueous solution. With increasing acid (H_2SO_4) concentration in aqueous solution, the $-NMe_2$ group of 2-MDMABA is protonated and this protonated form originates emission at ~499 nm with diminishing LE emission intensity. From the linearity of Benesi–Hildebrand plot of $1/(I-I_0)$ versus $1/[H_2SO_4]$ (inset of Fig. 8a) 1:1 complexation between probe and acid is confirmed. To find the orientation and the location of the target molecule inside the CDs cavity, the effect of decrease of pH on the emission of 2-MDMABA entrapped in CDs has been performed. Figure 8b shows that upon the addition of H_2SO_4 to 10 mM α-CD solution containing the probe, the LE emission intensity decreases with the formation of a new band at ~500 nm, similar to the case of water. In case of *β*- and *γ*-CD, the same results are obtained with the addition of small amount of acid (inset of Fig. 8b). These features can only be attributed to the fact that the donor part, i.e. $-NMe_2$ group sticks outside the cavity and exposed to the outside hydrophilic region and gets protonated in presence of mild acids. So 2-MDMABA forms 1:1 complex with two CDs and the locking phenomenon is caused with the donor $-NMe_2$ group protrudes outside.

Scanning electron microscopy of solid complexes

Scanning electron microscopy is used to asses the microscopic aspects of the host, guest and their inclusion

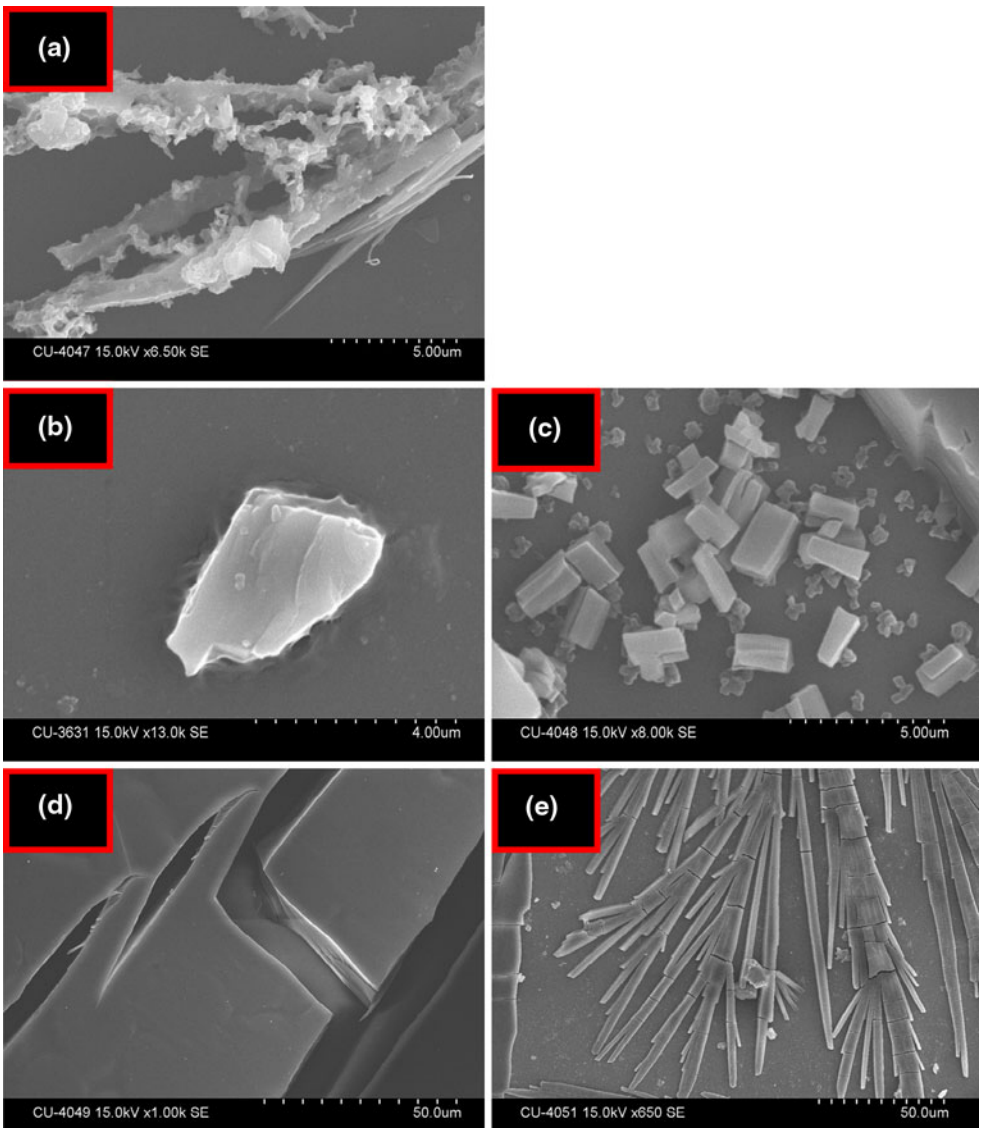

Fig. 9 SEM photographs of pure 2-MDMABA (**a**), α-CD (**b**), β-CD (**c**) and their corresponding inclusion complexes as α-CD + 2-MDMABA (**d**) and β-CD + 2-MDMABA (**e**)

complexes (Fig. 9). Even, if it is not a decisive method to confirm the inclusion phenomenon, nevertheless, it helps to asses the morphological changes of the crystals. It is possible to observe the needle-shaped morphology of 2-MDMAB (a) with a rough surface and smooth sheeted/plated structure of α-CD (b). Pure β-CD (c) also appears as agglomerates of crystalline particles with tabular shape. The corresponding materials obtained by complex formation methods, a new population of particles with different shape occur, which is not seen in the pure materials. In case of α-CD (d), the small layers of inclusion complexes are observed. The inclusion materials of β-CD (e) with the probe appear as rodlike or columnar structure with various diameter and no crystals from the pure 2-MDMABA or pure CD could be distinguished. So the SEM photographs demonstrate the interaction of 2-MDMABA with CDs by indicating a morphological change of the crystals in all the obtained materials compared to the pure starting materials due to the formation of an inclusion complex.

Conclusions

The ultimate goal of this study is to unravel the spectral modulation and orientation of a charge transfer probe 2-methoxy-4-(*N*,*N*-dimethylamino)benzaldehyde (2-MDMABA), encapsulated within different CDs in aqueous medium. The spectral behavior of this probe is modified significantly upon complexation with CDs of different cavity size. The increase of both LE and ICT emission is basically due to

lowering of the polarity of the medium. The Benesi–Hildebrand plot clearly indicates that while only 1:1 complexation occurs with β- and γ-CD, with α-CD both the 1:1 and 1:2 inclusion complexes are formed depending on the concentration of α-CD. SEM measurement also supports complexation between probe and CDs with different structural pattern. The data further suggests that β-CD binds strongly with 2-MDMABA whereas loose binding occur in case of γ-CD due to size mismatching. The increase in the fluorescence quantum yield value and decay times of the probe encapsulated within CDs cavity have been ascribed by the lowering of the non-radiative decay rates in these nanocages. The acid effect unequivocally establishes that in aqueous solution of CDs, the donor $-NMe_2$ group is projected outside while the acceptor -CHO group is entrapped within the hydrophobic part of the cyclodextrin cavity.

Acknowledgments This research is supported by DST, India (Project no. SR/S1/PC/26/2008). We appreciate the cooperation received from Prof. T. Ganguly IACS, Kolkata for his kind help in lifetime measurements. We are also thankful to A. Mallik and Dr. P. K. Maity, C. U., for their kind help in SEM measurements. AS and SJ thank CSIR and UGC for research fellowship.

References

1. Douhal, A.: Ultrafast guest dynamics in cyclodextrin nanocavities. Chem. Rev. **104**, 1955–1976 (2004)
2. Del Valle, E.M.M.: Cyclodextrins and their uses: a review. Proc. Biochem. **39**, 1033–1046 (2004)
3. Szetjli, J.: Cyclodextrins and Their Inclusion Complexes. Academic Kiado, Budapest (1982)
4. Szetjli, J.: Introduction and general overview of cyclodextrin chemistry. Chem. Rev. **98**, 1743–1753 (1998)
5. Drexler, K.E.: Nanosystems: Molecular Machinery Manufacturing and Computation. Wiley, New York (1992)
6. Al-Hassan, K.A., Khanfer, M.F.: Fluorescence probes for cyclodextrin interiors. J. Fluoresc. **8**, 139–152 (1998)
7. Szetjli, J.: Cyclodextrin Technology. Kluwer Academic Publishers, Dordrecht (1988)
8. Villalonga, R., Cao, R., Fragoso, A.: Supramolecular chemistry of cyclodextrins in enzyme technology. Chem. Rev. **107**, 3088–3116 (2007)
9. D'Souza, V.T., Bender, M.L.: Miniature organic models of enzymes. Acc. Chem. Res. **20**, 146–152 (1987)
10. Kim, Y., Yoon, M., Kim, D.: Excited-state intramolecular proton transfer coupled-charge transfer of p-*N*,*N*-dimethylaminosalicylic acid in aqueous β-cyclodextrin solutions. J. Photochem. Photobiol. A Chem. **138**, 167–175 (2001)
11. Bender, M.L., Komiyama, M.: Cyclodextrin Chemistry. Springer, New York (1977)
12. Hedges, R.A.: Industrial application of cyclodextrins. Chem. Rev. **98**, 2035–2044 (1998)
13. Saenger, W.: Cyclodextrin inclusion compounds in research and industry. Angew. Chem. Int. Ed. Engl. **19**, 344–362 (1980)
14. Paul, B.K., Samanta, A., Guchhait, N.: Modulation of excited-state intramolecular proton transfer reaction of 1-hydroxy-2-napthaldehyde in different supramolecular assemblies. Langmuir **26**, 3214–3224 (2010)
15. Mitra, S., Das, R., Mukherjee, S.: Intramolecular proton transfer in inclusion complexes of cyclodextrins: role of water and highly polar nonaqueous media. J. Phys. Chem. B **102**, 3730–3735 (1998)
16. Mukhupadhyay, M., Banerjee, D., Mukherjee, S.: Proton-transfer reaction of 4-methyl 2,6-diformyl phenol in cyclodextrin nanocage. J. Phys. Chem. A **110**, 12743–12751 (2006)
17. Al-Hassan, K.A., Saleh, N., Abu-Abdoun, I.I., Yousef, Y.A.: Inclusion as a driving force for the intramolecular charge transfer (ICT) fluorescence of p-(*N*,*N*-diphenylamino)benzoic acid methyl ester (DPABME) in α-cyclodextrin (α-CD) aqueous solution. J. Incl. Phenom. Macrocycl. Chem. **61**, 361–365 (2008)
18. Chakraborty, A., Guchhait, N.: Inclusion complex of charge transfer probe 4-amino-3-methyl benzoic acid methyl ester (AMBME) with β-CD in aqueous and non-aqueous medium: medium dependent stoichiometry of the complex and orientation of probe molecule inside β-CD nanocavity. J. Incl. Phenom. Macrocycl. Chem. **62**, 91–97 (2008)
19. Das, P., Chakrabarty, A., Haldar, B., Mallick, A., Chattopadhyay, N.: Effect of cyclodextrin nanocavity confinement on the photophysics of a β-carboline analogue: a spectroscopic study. J. Phys. Chem. B **111**, 7401–7408 (2007)
20. Singh, R.B., Mahanta, S., Guchhait, N.: Spectral modulation of charge transfer fluorescence probe encapsulated inside aqueous and non-aqueous β-cyclodextrin nanocavities. J. Mol. Struct. **963**, 92–97 (2010)
21. Hamai, S.: Pyrene excimer formation in gamma-cyclodextrin solutions: association of 1:1 pyrene-gamma-cyclodextrin inclusion compounds. J. Phys. Chem. **93**, 6527–6529 (1989)
22. Hamai, S., Hatamiya, A.: Excimer formation in inclusion complexes of β-cyclodextrin with 1-alkylnaphthalenes in aqueous solutions. Bull. Chem. Soc. Jpn. **69**, 2469–2476 (1996)
23. Chakraborty, A., Kar, S., Guchhait, N.: Photoinduced intramolecular charge transfer reaction in (*E*)-3-(4-methylamino-phenyl)-acrylic acid methyl ester: A Fluorescence Study in Combination with TDDFT Calculation. J. Phys. Chem. A **110**, 12089–12095 (2006)
24. Mahanta, S., Singh, R.B., Kar, S., Guchhait, N.: Photoinduced intramolecular charge transfer in methyl ester of *N*,*N*′-dimethylaminonaphthyl-(acrylic)-acid: spectroscopic measurement and quantum chemical calculations. J. Photochem. Photobiol. A Chem. **194**, 318–326 (2008)
25. Rotkiewicz, K., Grellman, K.H., Grabowski, Z.R.: Reinterpretation of the anomalous fluorescense of p-n, n-dimethylaminobenzonitrile. Chem. Phys. Lett. **19**, 315–318 (1973)
26. Kosower, E.M., Dodiuk, H.: Multiple fluorescences. II. A new scheme for 4-(*N*,*N*-dimethylamino)benzonitrile including proton transfer. J. Am. Chem. Soc. **98**, 924–929 (1976)
27. Samanta, A., Paul, B.K., Mahanta, S., Singh, R.B., Kar, S., Guchhait, N.: Evidence of acid mediated enhancement of photoinduced charge transfer reaction in 2-methoxy-4-(*N*,*N*-dimethylamino) benzaldehyde: Spectroscopic and quantum chemical study. J. Photochem. Photobiol. A Chem. **212**, 161–169 (2010)
28. Kawski, A., Kukliński, B., Bojarski, P.: Excited state dipole moments of 4-(dimethylamino)benzaldehyde. Chem. Phys. Lett. **448**, 208–212 (2007)
29. Samanta, A., Paul, B. K., Guchhait, N.: Reinvestigation of photoinduced intramolecular charge transfer reaction in *p*-dimethylaminobenzaldehyde by spectroscopic method and density functional theory (DFT) calculation. J. Lumin. **132**, 517–525 (2012)
30. Kundu, S., Chattopadhyay, N.: Twisted intramolecular charge transfer of dimethylaminobenzaldehyde in α-cyclodextrin cavity. J. Mol. Struc. **344**, 151–155 (1995)
31. Kundu, S., Chattopadhyay, N.: Dual luminescence of dimethylaminobenzaldehyde in aqueous β-cyclodextrin: non-polar and

TICT emissions. J. Photochem. Photobiol. A Chem. **88**, 105–108 (1995)
32. Fischer, M., Georges, J.: Fluorescence quantum yield of rhodamine 6G in ethanol as a function of concentration using thermal lens spectrometry. Chem. Phys. Lett. **260**, 115–118 (1996)
33. Mandal, P., Kundu, S., Misra, T., Roy, S.K., Ganguly, T.: Effects of liquid crystal environment on the spectroscopic and photophysical properties of well-known reacting systems 2,3-dimethylindole (DMI) and 9-cyanoanthracene (9CNA). J. Phys. Chem. A **111**, 11480–11486 (2007)
34. Frisch, M.J., et al.: Gaussian 03, Revision B.03. Gaussian, Inc, Pittsburgh (2003)
35. Lackowicz, J.R.: Principles of Fluorescence Spectroscopy. Plenum Press, New York (2006)